Irrigation Science
https://doi.org/10.1007/s00271-022-00791-1

ORIGINAL PAPER

Design and characterization of a pneumatic micro glass beads matrix sensor for soil water potential threshold control in irrigation management

Carlos Manoel Pedro Vaz[1] · Luiz Fernando Porto[2] · Carlos Ignácio D´Alkaine[3] · Luis Henrique Bassoi[1] · André Torre Neto[1] · Jan W. Hopmans[4] · Dennis E. Rolston[4]

Received: 1 October 2021 / Accepted: 15 February 2022

Abstract
Soil moisture porous matrix sensors may be good alternatives to tensiometers for measuring soil–water matric potential (SMP) for irrigation scheduling based on soil–water status approaches. The objective of this paper is to present and evaluate a new porous matrix sensor (IGstat) for detecting specific SMP thresholds for possible application in irrigation scheduling regulated by the SMP threshold concept. The IGstat sensor uses a non-sintered, glass bead microspheres (microGB) core and an outer ceramic cup, having larger air bubbling pressure (BP), to establish hydraulic contact with the soil. Pneumatic, optical, or electrical properties of the microGB porous medium can be then measured to infer the SMP. This paper describes and evaluates the performance of IGstat sensors for SMP threshold detection, using the pneumatic mode with a small air flow applied and air pressure monitored in the sensor tubing. Five IGstat sensors were built with different microGB diameters (15–125 µm) having air BP varying from 6 to 40 kPa. A power function was fitted to the data, which can be used to select microGB diameters to build IGstat sensors of required air BP. The experimental setup proposed to determine the sensor BP by incremental air injection provided air BP values in good agreement with those observed in a soil evaporation experiment (average relative error of 7.6%). The sensor responses in soil, with a small air pressure applied to them, showed a sharp pressure decreases when the SMP approached the sensor air BP, decreasing to about zero for SMP equal to the sensor air BP. The proposed sensors and approach showed potential for irrigation scheduling.

Introduction

Agriculture is the main user of freshwater globally, and for this reason efficient irrigation is of paramount importance. Efficient irrigation scheduling prevents plant water stress, improves yield and crop quality, minimizes losses by deep percolation, and decreases salinization and erosion (Müller et al. 2016; Nikolaou et al. 2020). The different types of irrigation scheduling can be classified into three main categories: soil-based (soil–water status measurements), plant-based (sensing of crop water stress), and weather-based (evapotranspiration and water balance measurements) approaches (Gu et al. 2020).

Soil-based irrigation techniques use soil–water matric potential (SMP) or soil–water content (SWC) sensors to monitor the water status during the growing season. Irrigation would be initiated whenever a lower level of SMP (more negative) or SWC (less positive) threshold is achieved, and irrigation stopped when an upper-level threshold (normally the field capacity) is reached (less negative SMP or more positive SWC). Some examples of such techniques can be found in Matteau et al. (2021a, b); Liu et al. (2021); Jabro et al. (2020); Gendron et al. (2018); Contreras et al. (2017); Oroosch et al. (2016); Nolz et al. (2016); Ganjegunte et al. (2012) and Wang et al. (2007). Threshold values can be obtained from previous studies (Bianchi et al. 2017; Müller et al. 2016; Taylor 1965) or provided by extension services, consultants, and suppliers (Thompson et al. 2007). However, as such values may vary among crops, cultivars, soil properties, crop systems, and location of the sensor and growth stage, usage of specific

✉ Carlos Manoel Pedro Vaz
carlos.vaz@embrapa.br

[1] Embrapa Instrumentation, São Carlos, SP, Brazil

[2] Tecnicer Tecnologia Cerâmica, São Carlos, SP, Brazil

[3] Centro Universitário Central Paulista, São Carlos, SP, Brazil

[4] University of California, Davis, CA, USA

Published online: 17 April 2022

threshold values determined for local conditions through field experiments is highly recommended (Gu et al. 2020; Müller et al. 2016; Thompson et al. 2007).

The application of SMP threshold is more straightforward than SWC threshold, because it is directly linked to the plant's ability to uptake water and is less dependent on soil type (Müller et al. 2016; Campbell and Campbell 1982). Soil–water matric potential can be determined directly by water-filled hydraulic tensiometers or indirectly by porous matrix SMP sensors using heat dissipation, dielectric permittivity, or resistivity methods (Jabro et al. 2020; Malazian et al. 2011; Flint et al. 2002). Although the conventional tensiometer is the standard tool for SMP determinations, there are limitations such as the relatively low working range (from 0 to about − 85 kPa) and the need for frequent maintenance (water refill) due to cavitation of water when the soil dries to values lower than the equivalent local barometric pressure (Whalley et al. 2013). For these reasons, a variety of matric potential sensors has been developed that are commercially available for several uses, including irrigation regulated by threshold (Matteau et al. 2021a, b; Nolz et al. 2016; Thompson et al. 2007). Bianchi et al. (2017) summarize the advantages and limitations of the porous matrix SMP sensors compared to conventional tensiometers. Main disadvantages of these sensors are related to calibration requirements and influence of temperature, and some devices have low accuracy for the wet range, are influenced by soil salinity, and are relatively expensive. Due to these limitations, the development of inexpensive, accurate, and maintenance free devices for SMP measurements in the field are still of great interest.

The SMP sensor developed by Calbo et al. (2013), named IGstat, works similarly to other porous matrix SMP sensors, but it uses a non-sintered, glass bead microspheres (microGB) core in which pneumatic, optical, or electrical properties can be measured to infer the SMP. An outer ceramic cup having a larger air bubbling pressure-BP (also referred to as breakthrough capillary pressure, threshold pressure or air-entry pressure) makes the hydraulic contact with the soil and prevents air to flow through the ceramic and to the soil when injected air is applied through the microGB core (pneumatic measuring mode; Fig. 1). In this mode, the sensor measures SMP from zero up to the air bubbling pressure of the microGB porous medium (Calbo et al. 2013). It is therefore that the operating range for this IGstat sensor is controlled by the size of the spherical glass beads and associated largest pore spaces between the beads.

The simplest and easiest operation mode for the IGstat sensor is the pneumatic threshold mode, obtained when a small air pressure (smaller than the bubbling pressure of the microGB core) is applied to the inflow tubing and the air pressure in the sensor is monitored periodically. In such mode, air will flow through the outflow tubing (Fig. 1) only when the soil dries to a SMP equal or smaller (more negative) than the air bubbling pressure of the microGB porous medium, and the air flow ceases when the soil wets again. Selecting microGB of different diameters provide IGstat sensors with different bubbling pressures. Working in this pneumatic threshold mode, the IGstat sensor may be useful for irrigation scheduling by designing sensors with bubbling pressures equal to the lower and upper SMP threshold values for different crops and conditions.

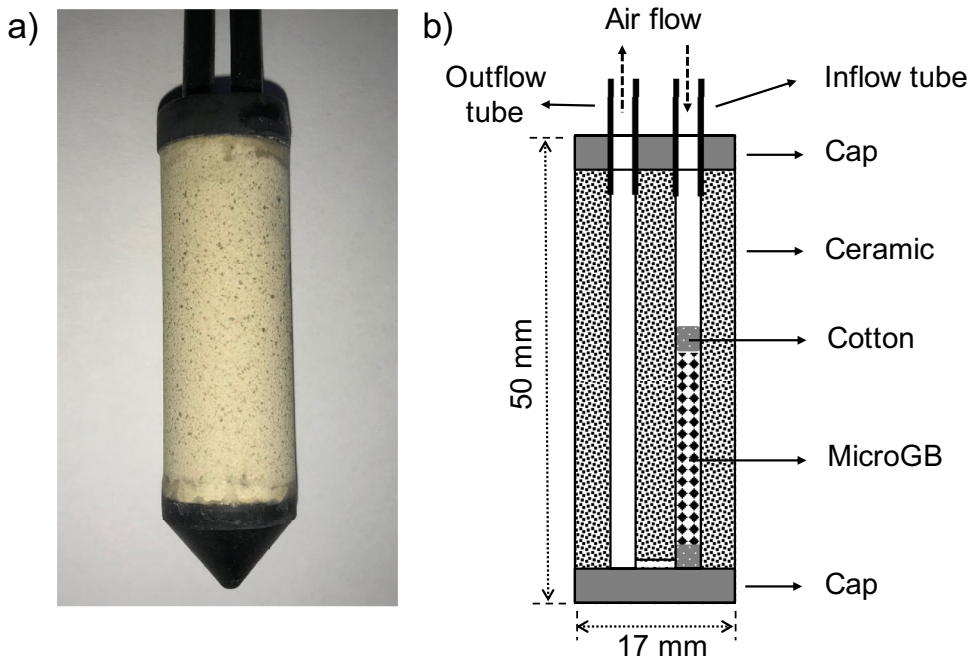

Fig. 1 The microGB matrix porous sensor IGstat (**a**) and a cross sectional view showing its parts and dimensions (**b**)

The air bubbling pressure of porous media can be determined by the air injection method, applying incremental air pressure steps (multi-step procedure) to displace the water phase by the gas phase in a saturated porous medium (Yokoyama and Takeuchi 2009; MacMullin and Muccini 1956; Thomas et al. 1968).

This paper evaluates the performance of IGstat sensors built with different microGB diameters (different air BP), working in the pneumatic-threshold mode (low air pressure input) for applications in irrigation regulated by the SMP threshold. The objectives are: (i) obtain an experimental relationship between microGB diameter and air bubbling pressure; (ii) evaluate the performance of the incremental air injection method for determining the sensor air bubbling pressure; and (iii) evaluate the sensor response in a soil during cycles of drying by evaporation, compared to that when using a tensiometer.

Materials and methods

For this study, five IGstat sensors were built with different microGB particle size distributions and their air BP and responses in soil were determined. This section describes the sensor design and its construction steps and presents the experimental procedures for the air BP determination and their evaluation in soil.

Determination of air bubbling pressure

MicroGB fractions were separated from soda-lime glass beads (Zirtec, São Paulo, Brazil) types AI (< 53 µm), AG (53–105 µm), or AF (74–149 µm) to build five IGstat sensors with different air bubbling pressures, to establish an experimental relationship between air bubbling pressure (BP) and microGB particle size. About 100 g of each microGB type (AI, AG, or AF) were shaken with distilled water in a low-speed reciprocal shaker (TE-160, Tecnal, Piracicaba, Brazil) during 2 h at 30 rpm, and then separated using a combination of sieving and sedimentation procedures, to produce about 10 g of each microGB diameter class. Particle size distribution of the microGB fractions was determined using a gamma-ray attenuation apparatus (Naime et al. 2001).

The air bubbling pressures of the IGstat sensors built with the five selected microGB fractions were determined using the incremental air injection method, according to the experimental setup shown in Figs. 2a and b. In this method, incremental air pressures were applied by an air pressure

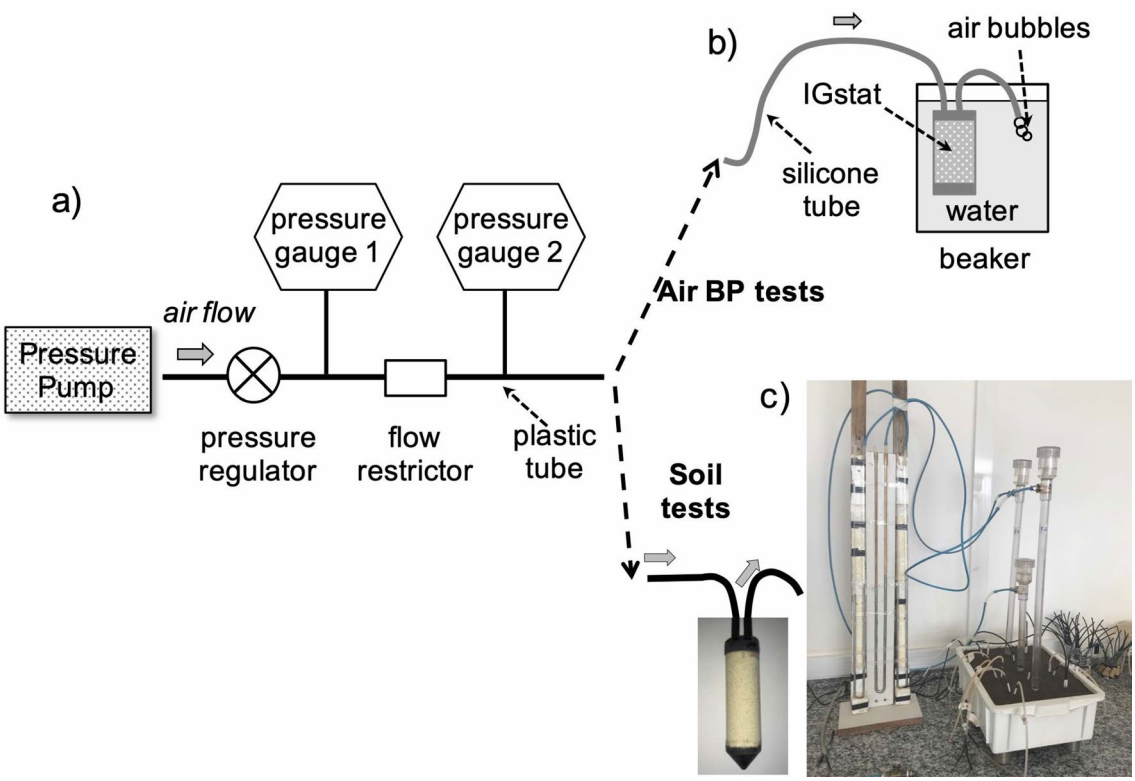

Fig. 2 Experimental setup for determining the air bubbling pressure of IGstat sensors using the incremental air injection method (**a**, **b**) and the measurements in soil (**a**, **c**). Measurements in soil are performed applying a small air flow/pressure (2.6 cm Hg) and measuring the pressure in gauge 2, after 3 min of equilibration time

pump (Q955P, Quimis, Diadema, Brazil) using a pressure regulator valve (gauge 1). The air pressure in the IGstat sensor was measured after 3 min (gauge 2), after equilibrium was attained, starting with a pressure value smaller than the sensor air BP and ending after some pressure steps when the input air pressure exceeded the sensor BP value (observed by air bubbles coming out from the sensor outflow tubing). The flow restrictor between gauges 1 and 2 aimed to reduce the air flow from a magnitude of liters per minute (produced by the air pump) to milliliters per minute, to more accurately monitor the sensor and to avoid disturbance of the glass beads.

IGstat sensor construction and soil evaluation

The IGstat sensors were constructed by mixing the microGB with water in a ceramic porous sleeve, and shaking the microGB (with water, to ensure settling of the porous mixture (Fig. 1b). After introducing hydrophilic cotton to keep the microGB material in place, two plastic caps were glued to the ceramic sleeve together with the plastic inflow and outflow tubing. All sensors were checked for air leaks. The outer ceramic BP was determined for each sensor using the setup presented in Figs. 2a and b, by closing the outflow tubing and forcing air to flow through the ceramic body, so as to confirm that the ceramics has a larger air BP than the microGB core. Prior to any subsequent soil installation or BP measurement, the sensor was submerged in water for at least two hours to ensure full saturation of the ceramics and microGB core.

To evaluate sensor response and its reproducibility, each IGstat sensor was installed in a plastic container with a Typic Apludox soil (0.34 g g^{-1} clay content) and evaluated for about 5 months. Three water-filled tensiometers (homemade) connected to a mercury manometer were installed to independently determine the true soil–water matric potential. After sensor installation, water was added to the soil surface until drainage occurred from the perforated bottom and allowed to evaporate, while measurements were taken twice daily (morning and afternoon). Measurements consisted of applying an input pressure of 3.47 kPa (2.6 cm Hg) to each IGstat sensor, using the setup shown in Fig. 2a and c, followed by measuring the pressure at gauge 2 after it stabilized (after about 3 min). The soil was re-saturated whenever it reached a SMP of about − 60 kPa, as measured by the water-filled tensiometer, completing 5 wetting/drying cycles in the evaluation period. The input air pressure was selected so it was smaller than the lowest measured sensor air BP, so that, the pressure in gauge 2 is equal to the input pressure (gauge 1) at near soil saturation. When the soil dries to a SMP smaller than (more negative) the sensor BP, the pressure measured at gauge 2 will be less than for gauge 1, and proportional to the SMP.

The IGstat pressure relationship with SMP exhibited a sigmoidal shape and was fitted with an equation alike that of van Genuchten (1980):

$$P_{\mathrm{IGstat}} = P_{\mathrm{r}} + \left(P_{\mathrm{i}} - P_{\mathrm{r}}\right)\left[\frac{1}{1+(a\Psi)^{b}}\right]^{\frac{b-1}{b}}, \quad (1)$$

where P_{r} (kPa) and P_{i} (kPa) are the adjusted residual and input air pressures, a (kPa^{-1}) and b (dimensionless) are shape coefficients for the sigmoidal type equation, ψ (kPa) is the soil–water matric potential, and P_{IGstat} (kPa) is the pressure measured of the IGstat sensor (gauge 2, shown in Figs. 2a and c). Equation 1 was fitted to all experimental data by non-linear least-squares fitting (Wraith and Or 1998) using the Solver tool of Excel (Microsoft, Redmond, USA).

Results and discussion

The particle-size frequency distributions (PSD) of each of the five microGB IGstat sensors are presented in Fig. 3 with their minimum, maximum, and modal values listed in Table 1. Although the particle fractionation procedure was intended to select microGB fractions with narrow diameter ranges, the PSD analysis showed relatively wide distributions, likely impacting sensor responses to changing SMP values. Specifically, we expect faster pressure drops for gauge 2 after the soil dries to a SMP value equal to the sensor air BP, as the microGB particle size diameter distribution becomes narrower.

Results of the air BP measurements using the incremental air injection method are presented in Fig. 4. For each sensor, when the applied air pressure approaches the sensor air BP, air flows through the sensor tubing and air bubbles will

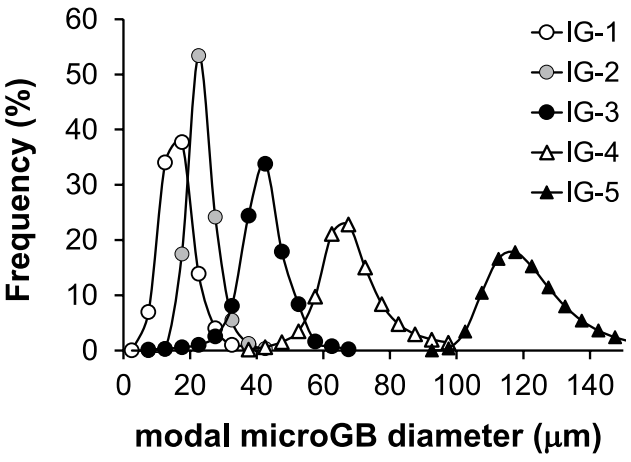

Fig. 3 Particle-size frequency distribution of the microGB fractions used to build the five IGstat sensors with different air bubbling pressures

Table 1 Minimum, maximum and modal diameter values of the five microGB fractions and air bubbling pressure (BP) of the IGstat sensors as determined with the incremental air injection method shown in Fig. 2

Sensor	MicroGB diameter (μm)			Air BP	d_{pore}
	Mode	Minimum	Maximum	(kPa)	(μm)
IG-1	15	5	30	39.7	7.3
IG-2	23	15	35	28.2	10.2
IG-3	42	25	55	17.1	16.8
IG-4	65	50	90	10.8	27.4
IG-5	125	100	150	5.7	50.5

d_{pore} pore diameter estimated by the capillary rise equation for water tensions equal to the measured air BPs

be observed when the outflow tube is immersed in water (Fig. 2a and b). The sensor BP is assumed to be equal to the applied pressure (gauge 1) when the first derivative of the line response changes from the 1:1 line on the graph between the applied air pressure and the air pressure measured in the sensor (gauge 2), as indicated by the arrows. Until the sensor response deviates from the 1:1 line, no air flows through the sensor since the pressure in the sensor is equal to the applied pressure. For applied pressures larger than the sensor BP, the pressures in the sensor are smaller than the applied pressures, because the air entry value of the sensor matrix will be exceeded so that air flows through the sensor. The slope of this response line for air pressures higher than the sensor air BP increases as the sensor BP increases (smaller microGB diameter and pore size). Such behavior is likely due to differences in the characteristic pore size of each sensor porous material in the material in the microGB core, reducing air permeability of the glass bead matrix permeability as its pore size decreases. According to Assouline and Or (2008), the air permeability of a porous medium permeability can be estimated from its air bubbling pressure and factors accounting for porosity, pore shape, and tortuosity effects.

The operating range of the IGstat sensors is defined by the particle and pore size of the microGB media, which defines the sensor air BP. Average pore size (diameter) for each microGB medium can be estimated using the capillary rise equation and the measured sensor air BP (Table 1). Pore size is defined by the particle size and packing. The relationship between the measured modal particle and the pore sizes gave a linear angular coefficient of about 0.4 that is characteristic of a stable packing arrangement in a pyramidal or tetrahedral geometrical configuration (Gupta and Larson 1979).

The experimental correlation between the sensor specific air BP and the particle diameters (modal values) were best fitted with a power type equation (Fig. 5). This mathematical relationship can be further used to design IGstat sensors of specific BP values between about 5 and 40 kPa. For larger BP values, microGB with modal diameters smaller than 15 μm shall be used. The air BP measuring time for each sensor was about 30 min. The proposed procedure (Fig. 2a and b) can be further automated for sensor standardization and quality control purposes.

The BP of the sensors ceramic body was also determined using the same experimental setup of Fig. 2a and b (keeping the outflow tubing closed), presenting an average value of

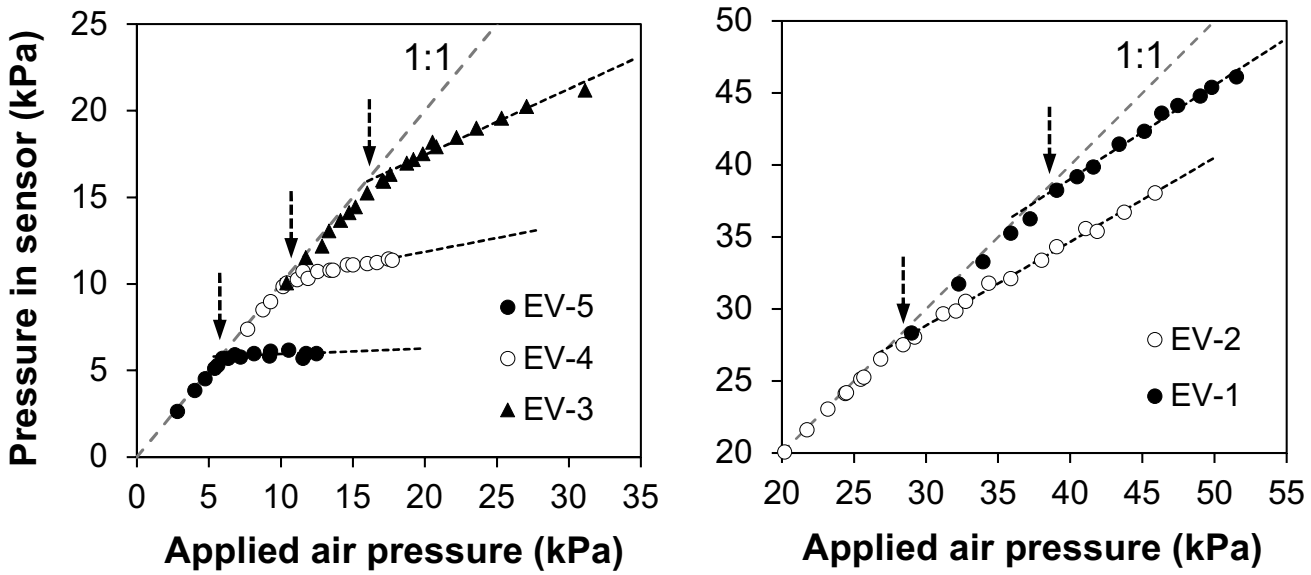

Fig. 4 Air pressure measured in the IGstat sensor (gauge 2) as a function of applied air pressure (gauge 1) using the experimental setup of Fig. 2a, b to determine the sensors air bubbling pressures (dashed vertical arrows) for sensors IG1 to IG5

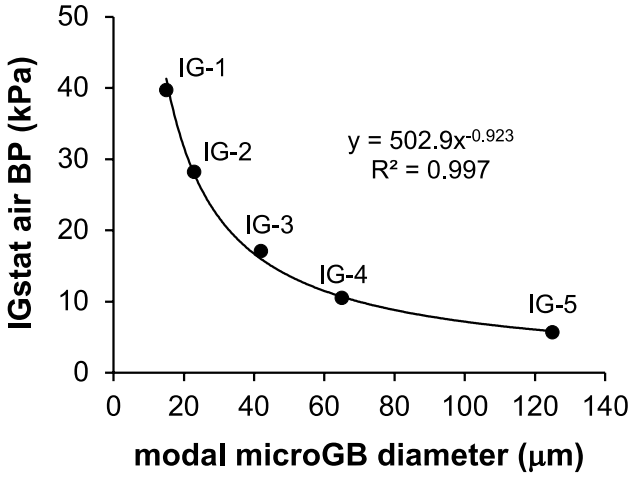

Fig. 5 Relationship between the air bubbling pressure measured for the five IGstat sensors of different microGB diameters (IG1 through IG5)

45 kPa, that was larger than the largest sensor air BP tested (IG-1; air BP: 39.7 kPa; modal microGB: 15 μm). Therefore, for the set of sensors evaluated, the ceramic body was adequate, but for IGstat sensors with BP larger than 40 kPa (modal microGB lower than 15 μm) it will be necessary to substitute the sensor ceramic material with those of larger air BP.

The incremental air injection method used to determine the sensor BP is essentially a direct gas injection into a saturated porous medium test, where the gas flow pattern can be either coherent or incoherent, depending on the medium pore size distribution (grain size and packing density) and gas injection rate (Geistlinger et al. 2006). Coherent gas flow refers to a continuous gas phase flow that follows Darcy's law, and incoherent gas flow means that the gas phase is discontinuously distributed. According to the criteria adopted by Geistlinger et al. (2006), the conditions used in the experiment (modal microGB diameters between 125 μm and 15 μm, and air flow rate from 3 to 130 mL min^{-1}, for the air BP tests carried out) provide a coherent flow pattern for the range of pressures, flow rates and pore sizes utilized.

The IGstat sensor response in soil (air pressure in gauge 2; Fig. 2a, c) presented a sharp decrease as the SMP decreased (more negative) and tended to a residual pressure (P_r of about 0.1 kPa) for SMP larger than the sensors BPs, as shown in Fig. 6a–e for each sensor individually and Fig. 6f for all sensors together. Solid lines represent Eq. (1) fitted to the experimental data, and vertical dashed lines indicate the sensors air BP measured with the incremental air injection method (Table 1). The largest measured air pressure in gauge 2 occurs when the soil is saturated or very wet and is equal

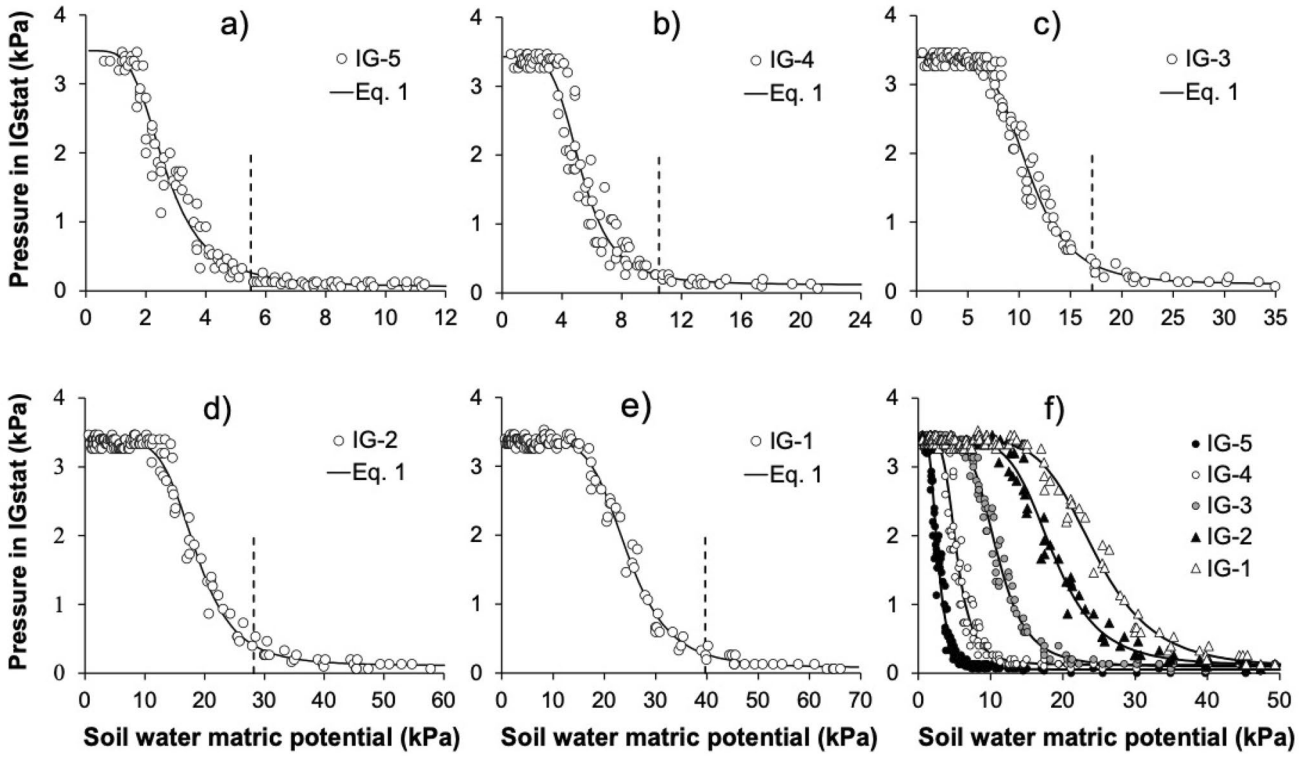

Fig. 6 Measured air pressure values at the IGstat sensor (pressure gauge 2) as a function of the soil–water matric potential (determined by water-filled tensiometers) for an input air pressure of 2.6 cmHg (3.47 kPa) and fitted with Eq. 1 (solid lines). Vertical dashed lines represent the sensor BP determined by the incremental air injection method

Table 2 Fitted parameters P_r, P_i, a, b (Eq. 1) for IGstat sensors responses with SMP (data of Fig. 6) and the root mean square error (RMSE) of the fittings

Sensor	P_r (kPa)	P_i	a (kPa^{-1})	b –	RMSE (kPa)
IG-1	0.1	3.37	0.042	6.35	0.19
IG-2	0.1	3.38	0.056	6.17	0.24
IG-3	0.1	3.39	0.096	5.75	0.14
IG-4	0.1	3.43	0.200	5.31	0.13
IG-5	0.1	3.48	0.411	4.39	0.11

P_i input air pressure, P_r residual air pressure, a, b shape coefficients

to the input pressure (gauge 1), since no air flows through the sensor tubing (Fig. 2a and c). When SMP approaches the sensor BP, pressure in gauge 2 decreases proportionally to the SPM and inversely to the microGB medium air permeability until a residual pressure close to zero and a maximum air permeability is achieved, resulting in the sigmoidal type responses shown in Fig. 6.

The fitted parameters to Eq. (1) are presented in Table 2. Coefficients a and b correlated linearly with the modal microGB diameter and non-linearly with the sensor air BP (Fig. 7a and b), whereas 1/a also related linearly to the sensor air BP (graph not shown). The linear relationships between the coefficients a and b with the modal microGB diameter can be used to predict the response of any IGstat sensor if its microGB particle-size frequency distribution is known for BP between 5 and 40 kPa.

To use the IGstat sensors in the pneumatic-threshold mode for controlling irrigation, it is necessary to define a reference air pressure value in the sensor (y axis in Fig. 6) to initiate the irrigation. Using as reference the sensor air pressure where SMP is equal to the BP gave air pressures of 0.27, 0.40, 0.39, 0.24, and 0.24 kPa for sensors IG-1 to IG-5, respectively. The average was 0.3 kPa, which is equivalent to a relative error of 7, 6% in air BP values compared to the air BP measured by the incremental air injection method. Therefore, for these sensors with an applied air pressure of 2.6 cm Hg, irrigation would be activated every time the pressure in gauge 2 reached 0.3 kPa, that is the moment that the soil–water potential approaches the specified sensor air BP.

The relationship presented in Fig. 5 can be used to build IGstat sensors of any BP between about 5 to 40 kPa by choosing the proper microGB diameter. Selecting IGstat sensors with BP equal to the upper and lower SMP threshold value of a given crop, allows applying the IGstat sensor for scheduling irrigation based on SMP threshold values.

Conclusions

A new soil water matric potential sensor, based on the sensor concept proposed by Calbo et al. (2013) is presented and evaluated. The experimental relationship between microGB diameter and air BP, and the method proposed here to determine the sensor air BP, provides a procedure to design IGstat sensors for use in irrigation regulated by SMP threshold (sensors with air BP equal to the lower and upper-level threshold). Based on the results obtained in the soil experiment, irrigation can be initiated when the air pressure in the sensor approaches zero (about 0.3 kPa for an applied pressure of 3.5 kPa) which is the moment the SMP reaches the sensor air BP value. Results indicate possible application of the IGstat sensor working in pneumatic mode for use in irrigation management. Further studies are necessary to extend the sensor operation range

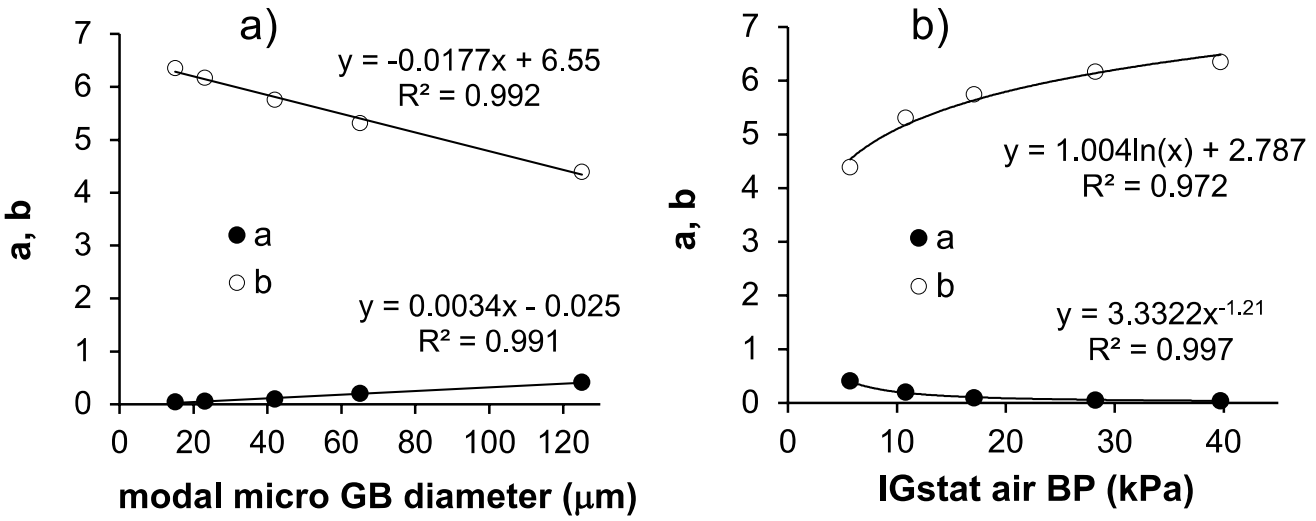

Fig. 7 Best linear and non-linear correlations between the fitted coefficients a and b (Eq. 1) and the IGstat microGB diameter (**a**) and the sensor BP (**b**)

for air BP larger than 40 kPa, which can be achieved using microGB diameters smaller than 15 µm, and to evaluate sensor-to-sensor variability and sensor performance for irrigation control, including comparisons with others commonly used SMP sensors.

Acknowledgements The authors thank FAPESP (2020/16179-3), EMBRAPA (30.21.90.041) for the financial support and Renê de Oste and José Ferrazini Júnior for the mechanic, hydraulic, and electronic support.

Data availability Data are available from the corresponding author upon request.

Declarations

Conflict of interest We declare that there are no financial, personal, and institutional conflicts of interest with the information and results presented in the article.

References

Assouline S, Or D (2008) Air entry-based characteristic length for estimation of permeability of variably compacted earth materials. Water Resour Res 44:W11403. https://doi.org/10.1029/2008WR006937

Bianchi A, Masseroni D, Thalheimer M, Medici LO, Facchi A (2017) Field irrigation management through soil water potential measurements: a review. Ital J Agrometeorol 2:25–38. https://doi.org/10.19199/2017.2.2038-5625.025

AG Calbo CMP Vaz WA Marouelli LF Porto 2013 Water tension sensor, system for characterizing and continuously measuring soil water system for indicating critical soil water tension and irrigation rod Patent Number: WO 2014172765 A1 2.

Campbell GS, Campbell MD (1982) Irrigation scheduling using soil moisture measurements: theory and practice. Adv Irrig 1:25–42. https://doi.org/10.1016/B978-0-12-024301-3.50008-3

Contreras JI, Alonso F, Cánovas G, Baeza R (2017) Irrigation management of greenhouse zucchini with different soil matric potential level. Agronomic and environmental effects. Agric Water Manag 183:26–34. https://doi.org/10.1016/j.agwat.2016.09.025

Flint AL, Campbell GS, Ellett KM, Calissendorff C (2002) Calibration and temperature correction of heat dissipation matric potential sensors. Soil Sci Soc Am J 66:1439–1445. https://doi.org/10.2136/sssaj2002.1439

Ganjegunte GK, Sheng Z, Clark JA (2012) Evaluating the accuracy of soil water sensors for irrigation scheduling to conserve freshwater. Appl Water Sci 2:119–125. https://doi.org/10.1007/s13201-012-0032-7

Geistlinger H, Krauss G, Lazik D, Luckner L (2006) Direct gas injection into saturated glass beads: transition from incoherent to coherent gas flow pattern. Water Resour Res 42:W07403. https://doi.org/10.1029/2005WR004451

Gendron L, Létourneau G, Anderson L, Sauvageau G, Depardieu C, Paddock E, van den Hout A, Levallois R, Daugovish O, Solis SS, Caron J (2018) Real-time irrigation: cost-effectiveness and benefits for water use and productivity of strawberries. Sci Hortic 240:468–477. https://doi.org/10.1016/j.scienta.2018.06.013

Gu Z, Qi Z, Burghate R, Yuan S, Jiao X, Xu J (2020) Irrigation scheduling approaches and applications: a review. J Irrig Drain Eng 146(6):04020007. https://doi.org/10.1061/(ASCE)IR.1943-4774.0001464

Gupta SC, Larson WE (1979) A model for predicting packing density of soils using particle-size distributions. Soil Sci Soc Am J 43:758–764. https://doi.org/10.2136/sssaj1979.03615995004300040028x

Jabro JD, Stevens WB, Iversen WM, Allen BL, Sainju UM (2020) Irrigation scheduling based on wireless sensors output and soil-water characteristic curve in two soils. Sensors 20:1336. https://doi.org/10.3390/s20051336

Liu H, Yin C, Gao Z, Hou L (2021) Evaluation of cucumber yield, economic benefit and water productivity under different soil matric potentials in solar greenhouses in north China. Agric Water Manag 243:106442. https://doi.org/10.1016/j.agwat.2020.106442

MacMullin RB, Muccini GA (1956) Characteristics of porous beds and structures. AIChE J 2(3):393–403. https://doi.org/10.1002/aic.690020320

Malazian A, Hartsough P, Kamai T, Campbell GS, Cobos DR, Hopmans JW (2011) Evaluation of MPS-1 soil water potential sensor. J Hydrol 402:126–134. https://doi.org/10.1016/j.jhydrol.2011.03.006

Matteau JP, Célicourt P, Létourneau G, Gumiere T, Gumiere SJ (2021a) Potato varieties response to soil matric potential based irrigation. Agronomy 11:352. https://doi.org/10.3390/agronomy11020352

Matteau JP, Célicourt P, Létourneau G, Gumiere T, Gumiere SJ (2021b) Potato varieties response to soil matric potential based irrigation. Agronomy 11:352. https://doi.org/10.3390/agronomy11020352

Müller T, Bouleaua C, Perona P (2016) Optimizing drip irrigation for eggplant crops in semi-arid zones using evolving thresholds. Agric Water Manag 177:54–65. https://doi.org/10.1016/j.agwat.2016.06.019

Naime JM, Vaz CMP, Macedo A (2001) Automated soil particle analyzer based on gamma ray attenuation. Comput Electron Agric 31:295–304. https://doi.org/10.1016/S0168-1699(00)00188-5

Nikolaou G, Neocleous D, Christou A, Kitta E, Katsoulas N (2020) Implementing sustainable irrigation in water-scarce regions under the impact of climate change. Agronomy 10:1120. https://doi.org/10.3390/agronomy10081120

Nolz R, Cepuder P, Balas J, Loiskandl W (2016) Soil water monitoring in a vineyard and assessment of unsaturated hydraulic parameters as thresholds for irrigation management. Agric Water Manag 164:235–242. https://doi.org/10.1016/j.agwat.2015.10.030

Osroosh Y, Peters RT, Campbell CS, Zhang Q (2016) Comparison of irrigation automation algorithms for drip-irrigated apple trees. Comput Electron Agric 128:87–99. https://doi.org/10.1016/j.compag.2016.08.013

Taylor SA (1965) Managing irrigation water on the farm. Trans ASAE 8:433–436

Thomas LK, Katz DL, Tek MR (1968) Threshold pressure phenomena in porous media. Soc Pet Eng J 8:174–184. https://doi.org/10.2118/1816-PA

Thompson RB, Gallardo M, Valdez LC, Fernandez MD (2007) Using plant water status to define threshold values for irrigation management of vegetable crops using soil moisture sensors. Agric Water Manag 88:147–158. https://doi.org/10.1016/j.agwat.2006.10.007

van Genuchten MT (1980) A closed form equation for predicting the hydraulic conductivity of unsaturated soils. Soil Sci Soc Am J 44:892–898. https://doi.org/10.2136/sssaj1980.03615995004400050002x

Wang FX, Kang Y, Liu SP, Hou XY (2007) Effects of soil matric potential on potato growth under drip irrigation in the north China plain. Agric Water Manag 88:34–42. https://doi.org/10.1016/j.agwat.2006.08.006

Whalley WR, Ober ES, Jenkins M (2013) Measurement of the matric potential of soil water in the rhizosphere. J Exp Bot 64(13):3951–3963. https://doi.org/10.1093/jxb/ert044

Wraith JM, Or D (1998) Nonlinear parameter estimation using spreadsheet software. J Nat Resour Life Sci Educ 27:13–19. https://doi.org/10.2134/jnrlse.1998.0013

Yokoyama T, Takeuchi S (2009) Porosimetry of vesicular volcanic products by a water-expulsion method and the relationship of pore characteristics to permeability. J Geophys Res Atmos 114:B02201. https://doi.org/10.1029/2008JB005758